Prediction shapes peripheral appearance

Matteo Valsecchi
Abteilung Allgemeine Psychologie, Justus-Liebig-Universität Giessen, Giessen, Germany

Jan Koenderink
Abteilung Allgemeine Psychologie, Justus-Liebig-Universität Giessen, Giessen, Germany
Experimental Psychology, KU Leuven, Leuven, Belgium
Experimental Psychology, Utrecht University, Utrecht, the Netherlands

Andrea van Doorn
Abteilung Allgemeine Psychologie, Justus-Liebig-Universität Giessen, Giessen, Germany
Experimental Psychology, KU Leuven, Leuven, Belgium
Experimental Psychology, Utrecht University, Utrecht, the Netherlands

Karl R. Gegenfurtner
Abteilung Allgemeine Psychologie, Justus-Liebig-Universität Giessen, Giessen, Germany

Peripheral perception is limited in terms of visual acuity, contrast sensitivity, and positional uncertainty. In the present study we used an image-manipulation algorithm (the Eidolon Factory) based on a formal description of the visual field as a tool to investigate how peripheral stimuli appear in the presence of such limitations. Observers were asked to match central and peripheral stimuli, both configurations of superimposed geometric shapes and patches of natural images, in terms of the parameters controlling the amplitude of the perturbation (*reach*) and the cross-scale similarity of the perturbation (*coherence*). We found that observers systematically tended to report the peripheral stimuli as having shorter reach and higher coherence. This means that their matches both were less distorted and had sharper edges relative to the actual stimulus. Overall, the results indicate that the way we see objects in our peripheral visual field is complemented by our assumptions about the way the same objects would appear if they were viewed foveally.

Introduction

Peripheral vision is characterized by a number of limitations compared to central vision (for reviews, see Rosenholtz, 2016; Strasburger, Rentschler, & Jüttner, 2011). Most prominently, contrast sensitivity for higher spatial frequencies declines as a function of eccentricity (e.g., Hilz & Cavonius, 1974; Johnston, 1987), but the ability to detect blur (e.g., Clarke, Green, & Chantler, 2012; Maiello, Walker, Bex, & Vera-Diaz, 2017; Wang, Ciuffreda, & Irish, 2006) and the ability to detect image distortions (Bex, 2010) are reduced as well. This indicates that in peripheral vision we cannot access a large part of the information on which the sharp and precise representation of our central visual field is based. This is aggravated by the fact that crowding further hampers our ability to correctly identify peripheral details in the presence of other nearby elements (for reviews, see Levi, 2008; Whitney & Levi, 2011).

Despite this pervasive anisotropy in our visual system, we do not continuously experience dramatic changes in the appearance of our visual world as we move our eyes. A number of mechanisms contribute to this impression of continuity, including the integration of pre- and postsaccadic information (Ganmor, Landy, & Simoncelli, 2015; Herwig, 2015; Wolf & Schütz, 2015), transsaccadic learning of the association between peripheral and central appearance (Bosco, Lappe, & Fattori, 2015; Herwig & Schneider, 2014; Herwig, Weiß, & Schneider, 2015; Valsecchi & Gegenfurtner, 2016; Weiß, Schneider, & Herwig, 2014), and extrapolation of foveal content to the peripheral visual field (Otten, Pinto, Paffen, Seth, & Kanai, 2016; Toscani,

Citation: Valsecchi, M., Koenderink, J., van Doorn, A., & Gegenfurtner, K. R. (2018). Prediction shapes peripheral appearance. *Journal of Vision*, *18*(13):21, 1–14, https://doi.org/10.1167/18.13.21.

https://doi.org/10.1167/18.13.21 Received July 3, 2018; published December 28, 2018 ISSN 1534-7362

Gegenfurtner, & Valsecchi, 2017). Transsaccadic learning and foveal extrapolation are two key elements that inform the construction of appearance in the peripheral visual field. A potential third key element is the extrapolation of visible peripheral input beyond the available information. An example is the phenomenon of sharpness overconstancy (Galvin, O'Shea, Squire, & Govan, 1997; Galvin, O'Shea, Squire, & Hailstone, 1999), in which peripherally displayed blurry edges are seen as sharp. This has been interpreted as an indication that the visual system integrates the degraded input in peripheral vision with a template for sharp edges—or, in other words, that the visual system interprets the presence of an edge in the visible spatial frequencies as evidence for the presence of an edge in the missing and invisible spatial frequencies.

Understanding how pervasive these mechanisms are and how they are integrated to produce the appearance of the peripheral field in our visual environment is a difficult task. The problem is to measure peripheral appearance in the first place. Historical approaches have included verbal reports (Lettvin, 1976; Metzger, 1936, 2006) and reproduction tasks, whereby observers are asked to draw what they saw in the periphery (Metzger, 1936, 2006). Drawing tasks have been used successfully to investigate the appearance of relatively simple stimuli (Baldwin, Burleigh, Pepperell, & Ruta, 2016; Coates, Wagemans, & Sayim, 2017; Sayim & Wagemans, 2017) and even of complex stimuli relying on highly trained observers (Sayim, Myin, & Van Uytven, 2015). Untrained observers cannot be expected to reproduce anything more complex than simple line drawings. The difficulty of understanding the effect of peripheral viewing on appearance based on drawings also increases as the stimuli become richer because the number of ways in which a drawing can differ from the template increases. The alternative is to have observers adjust or compare central and peripheral stimuli along some visual dimension until their appearance is equivalent. Again, this is relatively straightforward for simple stimuli and manipulations, for instance when comparing relative size (Newsome, 1972; Valsecchi & Gegenfurtner, 2016), brightness (Toscani et al., 2017), or numerosity (Valsecchi, Toscani, & Gegenfurtner, 2013). When dealing with more complex stimuli it becomes necessary to have more powerful tools, which can be used flexibly and can modify the images based on a representation inspired by the way our visual system represents the visual field, specifically in a scale space.

One such tool that has been used to successfully investigate peripheral vision is the texture-synthesis model of Portilla and Simoncelli (2000). In this model, textures are encoded as a large number of constraints that define the statistics of the scale decomposed image in a translation-invariant fashion. Within the model, pooling the descriptors over smaller or larger areas can simulate the effect of resolution loss, crowding, and positional uncertainty in peripheral vision (Balas, Nakano, & Rosenholtz, 2009; Keshvari & Rosenholtz, 2016), and this approach has been used to construct stimuli that are presumed to be indistinguishable when viewed peripherally (Freeman & Simoncelli, 2011; but see Wallis, Bethge, & Wichmann, 2016). The strength of the algorithm by Portilla and Simoncelli (2000) is that it apparently does a very good job at modeling peripheral vision for texturelike stimuli. For instance, it can be used to simulate the effect of peripheral viewing on numerosity perception (Balas, 2016; Valsecchi et al., 2013) and on the appearance of materials (Keshvari & Wijntjes, 2016). One limitation of the model is that it is based on modifying pure noise or the combination of pure noise and a sample image until it corresponds to the constraints of a given image, pooled over a certain spatial extent. This makes it complicated to predict the outcome of the algorithm a priori when the descriptors change slightly. This in turn means that it is difficult to use such a model to investigate the appearance of peripheral stimuli, for example in a matching task. If the observer cannot create an intuitive model of how manipulating a parameter affects the appearance of the stimulus, it becomes difficult to match its value across stimuli. A second limitation of the model is that it has mostly been developed as a texture-synthesis algorithm, providing the best results when applied to stimuli which are in essence defined at an intermediate scale, such as repeating patterns or surfaces.

An algorithm that overcomes both problems is the Eidolon Factory (Koenderink, Valsecchi, van Doorn, Wagemans, & Gegenfurtner, 2017). This algorithm is also based on a scale-based representation of the image, but instead of taking the approach of constraining noise toward a translation-invariant representation of the stimulus, it takes the opposite approach of applying local spatial distortions to the representation itself (for a detailed comparison of the two approaches, see Koenderink et al., 2017, appendix C). Notice that using a scale-space representation is a desirable quality for a tool that is meant to mimic perceptual effects. On the one hand, the human visual system is characterized by neurons with varying receptive-field size, which by definition implies that it represents the visual input at different scales. On the other hand, a scale-space representation has proven to be a solid base for algorithms simulating visual functions, such as the detection of salient input (e.g., Itti & Koch, 2000). Furthermore, the relative weight of sub-band content can deeply affect the appearance of materials and shape (e.g., Boyadzhiev, Bala, Paris, & Adelson, 2015; Giesel & Zaidi, 2013). The Eidolon Factory works by spatially warping the representation at each scale based on a random vector field, before the warped scale compo-

nents are recomposed to produce the eidolon. Random vector fields are generated by separately defining the X and Y components as Gaussian white noise convolved with a Gaussian filter. The random field which is used to warp a given scale results from the weighted combination of a field generated independently for that scale and an additional field which is shared by all scales. The outcome of the Eidolon Factory is determined by a limited number of parameters that affect the nature of the spatial distortion which is applied to the input image representation. The first, which we named *reach*, defines the standard deviation of the distribution of the random fields. The second parameter, *coherence,* defines the relative weight of the common displacement field shared by all scales and of the displacement fields computed independently for each scale. A coherence value of 0 corresponds to completely independent warping between scales, and a value of 1 corresponds to identical warping applied to all scales. Perceptually, an increase in reach is associated with increased distortion—for example, bending of edges, or inflation or compression of local features. A decrease in coherence is associated with the independent diffusion of edges across scales, so that they become fuzzy and less defined. Notice that we choose to define this parameter as coherence in order to be consistent with our previous work (Koenderink et al., 2017). Its polarity, however, is arbitrary; we could have defined it as *incoherence,* associating the value 1 with maximum fuzziness.

Finally, a third parameter which we called *grain* controls the behavior of the Eidolon Factory. Grain stands for the standard deviation of the Gaussian spatial filter which is convolved with the noise fields. It thus controls how spatially correlated the warping is. Extremely low values of grain, coupled with large enough values of reach, can make objects disaggregate into small fragments, whereas very high values of grain (relative to the size of the elements in the scene) can transform the warping from local to regional to a general translation of the image in a random direction. The role of grain is definitely relevant to peripheral vision. In particular, it is very likely that low grain will mask the visibility of distortions in the peripheral visual field, although high grain will mask the distortions altogether. However, considering that the perceptual effects of grain—in combination with reach and with the scale of the objects in the image—are most likely nonlinear, testing its effect will require a careful characterization of appearance in the different subsections of the parameter gamut.

In this first study we decided to concentrate on the reach and coherence parameters of the Eidolon Factory when using it as a tool to investigate the appearance of visual stimuli in the peripheral visual field. This allowed us to keep the dimensionality of the parameter space that we explored to a level that was manageable experimentally. We also chose to manipulate all the scales at the same time, although the architecture of the Eidolon Factory allows the targeting of a specific scale or a range of scales. We had observers match central and peripheral stimuli along dimensions defined in the parameter space of the Eidolon Factory. We found that observers generally tended to report the peripheral stimulus as having larger coherence and smaller reach compared to the values that were used to produce it. This is in agreement with the idea that given our inability to detect spatial distortions and to detect whether the finer and coarser structure of the image are spatially registered in peripheral viewing, our visual system constructs the appearance of a peripheral visual field as if stimuli were undistorted and edges sharp.

Methods

Observers

Twelve observers (nine women, three men; mean age = 26.5 years) took part in the matching experiment with artificial stimuli. Thirteen observers (eight women, five men; mean age = 26.3 years) took part in the matching experiment with natural stimuli. Eleven observers (eight women, three men; mean age = 24.8 years) took part in the discrimination experiment, but three were excluded from the analysis. The reason for the exclusion was that the threshold value returned by the fit was outside of the parameter gamut—that is, lower than 0 or higher than 100—on at least one of the axes. This indicates that those participants were unable to do the task.

All participants were unaware of the purpose of the study and provided written informed consent in agreement with the Declaration of Helsinki. The study protocol was approved by the local ethics committee at the University of Giessen (LEK FB6 2017-08).

Stimuli: Base stimuli

All stimuli used in the present study were transformed using the Eidolon Factory starting from a set of 100 artificial and 100 natural base stimuli. The artificial stimuli were 100 configurations of superimposed geometric shapes (Figure 1). Each configuration was in principle composed of a rectangle, an oval, a triangle, and an irregular quadrangle, although one of the shapes could be completely occluded by the others. While the geometric configurations were generated randomly, we selected only configurations where the average distance of the occupied pixels from the center

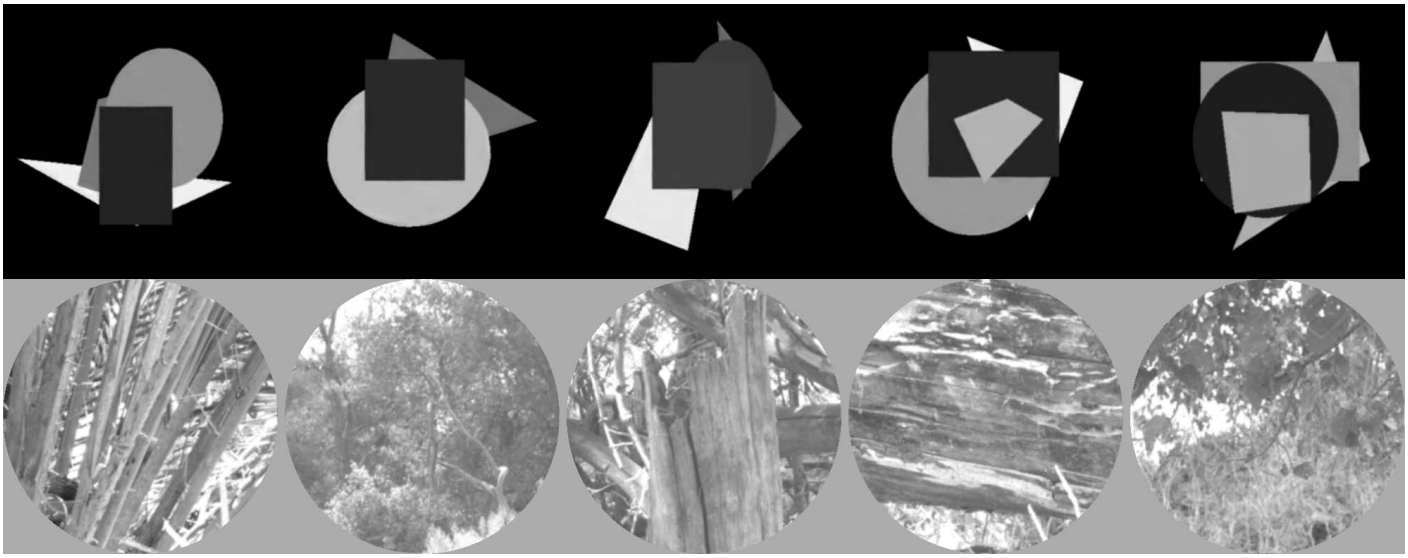

Figure 1. Examples of artificial (upper row) and natural (lower row) base stimuli.

was under 90 pixels, ensuring that the configurations were relatively compact. Once shown on the experimental display, the stimuli had an average cross section of 12°. The average luminance and the average SD contrast within the configurations were 32.5 and 27.5 cd/m^2, respectively.

The natural base stimuli were 100 grayscale circular patches (15.1°—i.e., 390-pixel diameter) taken from the UPenn Natural Image Database (Tkačik et al., 2011) after removing images of overlapping scenes. In order to make it possible for observers to match the degree of alteration produced on different images by the Eidolon Factory, it was necessary to ensure that the patches were very similar in their contrast and spatial-frequency content, given that the perceptual effect of applying a given random displacement to the image depends on the presence of fine-grained structures, and of course the detectability of distortion is bound to depend on contrast in the first place. After normalizing the average luminance within the patch to 57.6 cd/m^2 and the SD contrast to 50 cd/m^2 and excluding patches where more than 5% of the pixels overflowed the gamut of the monitor, we proceeded to select patches of relatively uniform histogram profile and power spectrum. This was done in a multistep process. First we computed the histograms and power spectra from 400 random patches. Then for each patch and bin of the histogram and of the power spectrum, we computed a z score relative to the distribution of the values in all 400 patches. Then for both the histogram and the power spectrum, we computed the distribution of the sum and of the maximum of the absolute z scores. The final patches were selected as being within the 32nd percentile of each of the four distributions.

Stimuli: Eidolon Factory

All stimuli were produced using the Eidolon Factory. All stimuli were constructed with a fixed grain of 12 pixels (0.47°) and different levels of coherence (100 steps between 0 and 100%) and reach (100 steps between 0 and 33.2 pixels—i.e., 1.3°—for the artificial images and between 0 and 7.7 pixels—i.e., 0.3°—for the natural images) combined according to specific directions in parameter space (see Figures 2 and 4). The lower reach range for the natural images was chosen because, subjectively, we had the impression that the quality of the images was degraded at much lower reach when compared to the artificial images, given their more complex structure. All stimuli used in the experiment were precomputed and were used for all observers. An impression of the effect of manipulating reach and coherence on the appearance of the stimuli can be obtained from Figure 2.

Display and eye-movement recording

Stimuli were presented on a 22-in. Eizo CG245W 10-bit LCD monitor (Eizo Corporation, Hakusan, Japan) at a viewing distance of 40 cm. Eye movements were recorded at 500 Hz with an EyeLink II system (SR Research, Missisauga, Canada).

Procedure: Matching task

In the matching task observers were shown two stimuli, one left and one right of the monitor center, always created by starting from different base stimuli of the same category. Their task was to change one

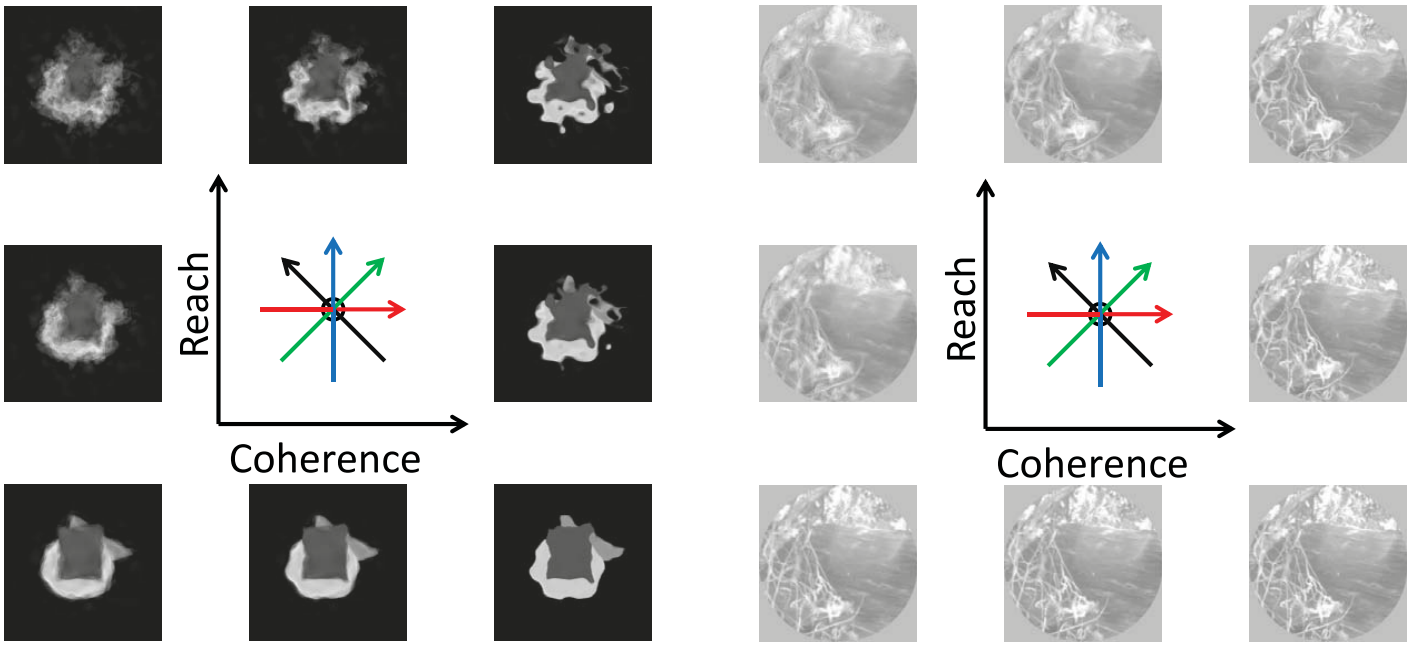

Figure 2. Eidolon Factory parameter space for an example artificial and natural image. Steps 20, 50, and 80 are depicted. The gamut extended from 0 to 100 for both parameters. Notice that high coherence is associated with sharper edges, low coherence is associated with fuzzy edges, and high reach is associated with increased distortion. The four arrows indicate the directions in the parameter space that were tested in the matching experiment.

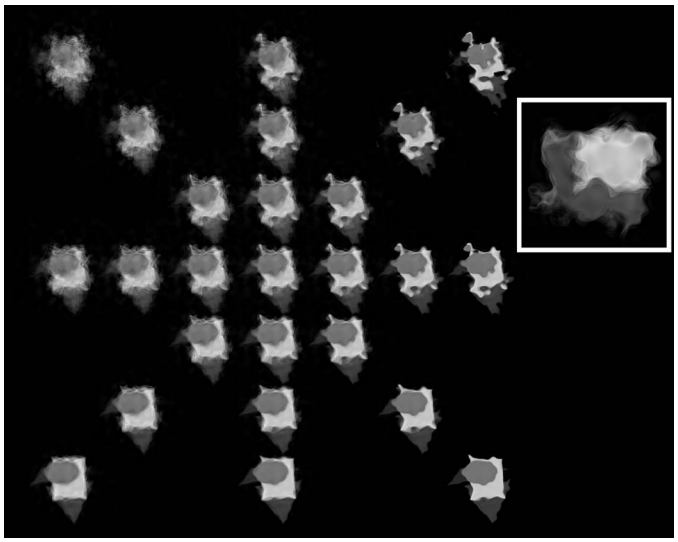

Figure 3. Matching procedure. Observers used the up and down arrow keys to move along one axis of the parameter space (multiple instances on the left, using the same spatial arrangement as Figure 2) in order to match the apparent distortion of a reference stimulus (enlarged stimulus in the square). As the observers pressed the up or down key, the stimulus morphed smoothly from one extremum of the gamut to the other. The reference stimulus has a parameter configuration corresponding to the center of the ranges (50 reach and 50 coherence—that is, fixed stimulus).

(randomly left or right in different trials) of the stimuli using the up and down arrow keys until the stimuli appeared equally modified (Figure 3). The initial value of the stimulus that had to be adjusted was chosen randomly among the 100 steps that defined the direction along which the matching took place. Notice that since we split the gamut into 100 steps, pressing the button produced a smooth morphing of the stimulus as the parameter(s) changed. There was no time limit for performing the match, and observers pressed a third key to signal that the procedure was over and to continue to the next trial. In different trials, observers modified only

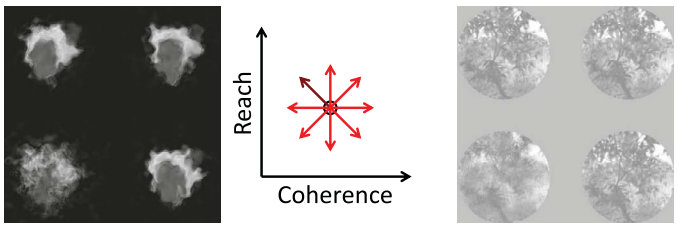

Figure 4. Example stimuli for the four-alternative forced-choice discrimination task. Observers saw four instances of eidolons from the same base stimulus and had to press one of four keys to indicate the odd one (bottom left in this case). Discrimination thresholds relative to the fixed distortion level (black circle in the central panel) were computed for each of the eight possible directions in the parameter space (red arrows). These examples depict an increase in reach associated with a decrease in coherence (up-left direction, darker color).

the reach parameter, only the coherence parameter, or combinations of the two, according to four possible directions in parameter space (see Figure 2). In the first block of trials, observers were free and encouraged to look at both stimuli, and the stimulus center-to-center distance was 20°. In the following block of trials, observers were forced to look at the stimulus they modified (the foveal stimulus) and to view the unchanging stimulus peripherally using a gaze-contingent paradigm, whereby the whole display disappeared as soon as the observer gazed further than 10° away from the center of the stimulus area. The choice of such a large tolerance was meant to limit the time the stimulus was blanked and to ensure that the eye movements within the foveal-stimulus area were not more restricted in the peripheral matching conditions as compared to the free-viewing condition. Indeed, fixations clustered mostly at the center of the stimulus that was being modified, with a horizontal distribution that closely matched the one that we observed in the free-viewing condition. Nonetheless, given that our stimuli were relatively extended, the effective eccentricity of the peripheral stimulus could be considerably less than the center-to-center distance, which was 20° or 30° in different trials of the second block.

The rationale of having a relatively liberal fixation check was also to limit the possible impact of adaptation on peripheral visibility. Despite the fact that on average observers took 9.4 s to complete each match, they executed saccades larger than 1° more than once per second and saccades larger than 2° approximately every 2 s, the most frequent amplitudes being 1.9° for the artificial-stimuli experiment and 0.6° for the natural-stimuli experiment. Generally speaking, those values seem more in line with free viewing an image of around 8° size rather than with the saccadic amplitudes and frequencies that one would expect during steady fixation (Otero-Millan, Macknik, Langston, & Martinez-Conde, 2013); and the presence of such large eye movements is expected to counteract the impact of adaptation on appearance (Martinez-Conde, Macknik, Troncoso, & Dyar, 2006; Mostofi, Boi, & Rucci, 2016).

Observers performed 192 matching trials in total in the artificial-stimuli experiment. All trials followed the same procedure, and observers were required to perform the same task. In the definition of our experimental design, trials were divided into 72 fixed-stimulus trials and 120 variable-stimulus trials, based on the parameter values that defined the peripheral stimulus. In the fixed-stimulus trials, the peripheral stimulus was always constructed using parameter values centered in the middle of the range, whereas in the variable-stimulus trials, the parameter values defining the peripheral stimulus changed from trial to trial. The fixed-stimulus trials were meant to measure a possible bias in the matched parameters between central and peripheral vision. For this purpose we used the stimulus that was centered in the parameter gamut and thus least likely to produce artifactually biased estimates. The variable-stimulus trials had two functions. First of all, they were meant to act as catch trials, ensuring that the observer experienced some degree of variation in the peripheral stimulus and thus was not just relying on memory to perform the task. Second, they gave us the possibility to check that observers were able to perform the task—that is, that their central matches were adjusted to the varying peripheral stimuli. While the parameter values for the variable-stimulus trials in the artificial-stimulus experiment were chosen randomly from the whole 100 steps of the range, in the case of the natural-image experiment they spanned 12 equally spaced values between steps 10 and 90. The trials were equally divided among all four directions and all three viewing conditions (free viewing, 20°, and 30°). The number of trials was increased to 288 in the natural-image experiment, with 144 fixed- and 144 variable-stimulus trials. Again, the trials were equally divided among all four directions and all three viewing conditions.

Procedure: Discrimination task

The discrimination task was conducted without eye tracking and in free viewing. In each trial, four instances of eidolons based on the same base stimulus were shown in the four quadrants of the screen, with a horizontal and vertical center-to-center distance of 20° (Figure 4). Observers pressed one of four keys to indicate which stimulus differed in distortion level from the others. Three of the stimuli were constructed using parameter levels at the center of the ranges, as in the fixed-stimulus trials in the matching experiments, whereas the fourth stimulus, located randomly in one of the four quadrants, was produced using parameter values located on one of eight possible directions of the parameter space (Figure 4, central panel). The eight directions were tested in separate blocks of 60 trials each, and each block was preceded by a practice session in which observers were given feedback to ensure that they knew what type of difference they were to expect in the following trials. We used an adaptive staircase method in order to present stimuli within the dynamic range for each observer and dimension.

Results

Matching task: Variable-stimulus trials

The first question is of course whether observers were able to perform the task of matching the

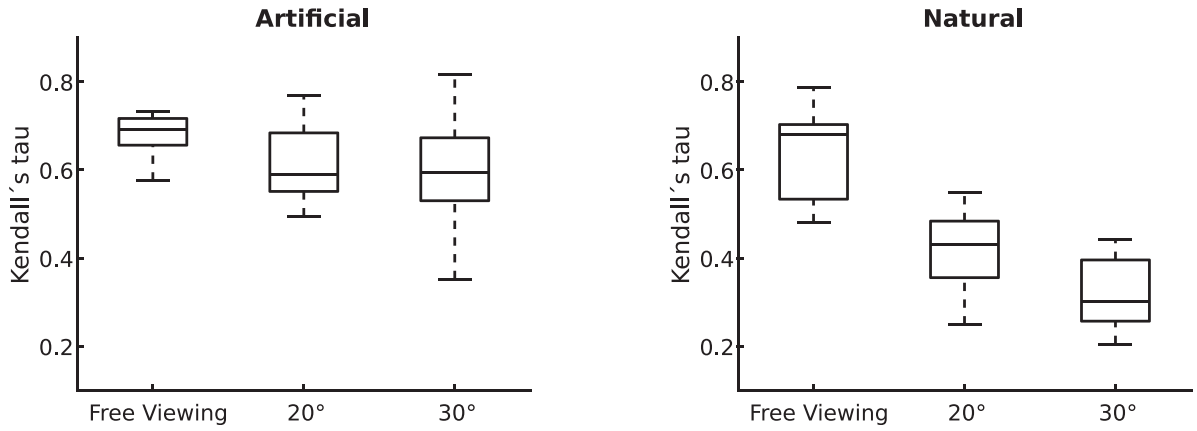

Figure 5. Distribution of correlation coefficients between sample and matched parameter values in variable-stimulus trials for artificial and natural stimuli. The values are lower for peripheral viewing and for natural images, but the fact that the correlations are generally positive indicates that observers were able to perform the task.

appearance determined by the eidolon parameters. In order to determine whether this was the case or not, as a first step we measured the correlation between the parameter values of the sample stimulus and the parameter values of the observers' matches in the variable-stimulus trials. This was done for each observer and viewing condition by collapsing the data across the four directions. Given that we cannot guarantee that the perceptual effect of the eidolon parameters is linear, we opted as much as possible for nonparametric tests, meaning that we only made the more conservative and plausible assumption that the relationship between parameter values and perception is monotonic. The distribution of Kendall's tau rank-correlation coefficients is depicted in Figure 5. While the correlation coefficients are lower for peripheral viewing and for the natural stimuli, the coefficients were invariably positive for each observer and condition, indicating that under all conditions observers were able to some extent to detect differences between the stimulus appearance in different trials and adapt their adjustments consequently.

Matching task: Fixed-stimulus trials

Given that the data from the variable-stimulus trials indicated that observers were able to perform the task, we can now answer the fundamental question of how complex stimuli appear in the periphery. The answer is based on the results of the fixed-stimulus trials, where the sample stimulus was repeatedly chosen from the central value of the Eidolon Factory parameter space. The parameter values obtained from the matches are shown in Figure 6. The first important observation is that the match values in the free-viewing condition correspond to the sample values, with the exception of the case where the parameters changed in a correlated fashion—that is, both increased or both decreased (green direction). This indicates that the matching procedure per se was precise and unbiased. As the sample stimulus is viewed peripherally, the observers tend to develop consistent biases, which are generally speaking in terms of increased coherence or decreased reach—that is, they tend to report the peripheral stimulus as being less distorted and less fuzzy than it actually was. If there were no bias, all symbols would be in the center, as they are approximately in the free-viewing case. The data are shifted, and the directions are towards lower reach and more coherence. When reach and coherence are traded off, observers seem to produce biased matches already when both stimuli are viewed foveally, particularly with natural images.

In order to verify precisely which biases were statistically significant, we compared the match values for free and peripheral viewing by means of Wilcoxon paired signed-rank tests. The results are presented graphically in Figure 6 and numerically in Table 1. The results of the analysis indicate that for both image types and both eccentricities, observers matched the peripheral stimulus with higher coherence and lower reach relative to free viewing when they manipulated both parameters in an anticorrelated way. A significant reduction was observed when reach alone was modified only in the case of natural images. The increase in coherence when it was modified in isolation was observed for artificial stimuli at both eccentricities and for natural stimuli only at 20°. No significant effects were observed when the two parameters were modified in a correlated way.

Discrimination task

The results from the matching experiment seem to indicate that no clear biases for peripheral matching

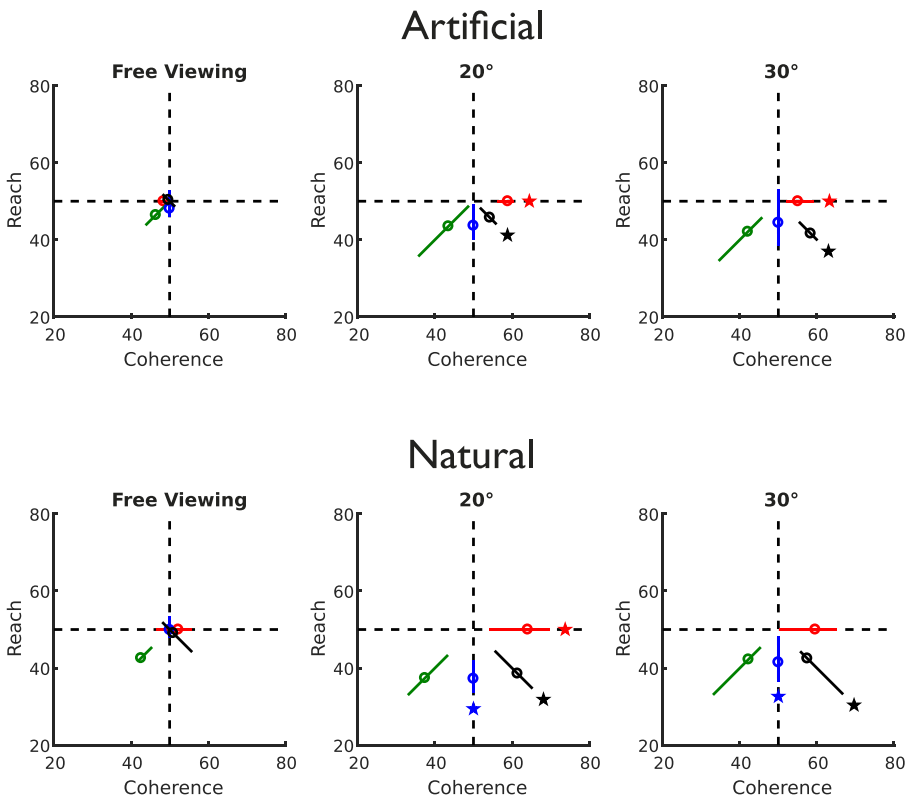

Figure 6. Match values for all four directions and both types of stimuli. Values are expressed in steps relative to the 100 steps that constitute the gamut for the adjustment. The lines represent the 25th and 75th percentiles of the individual-observer values; the circles represent the median value. Stars denote a significant difference ($p < 0.05$ after false-discovery-rate correction) between free viewing and peripheral viewing. If observers were unbiased in their matches independent of viewing condition, all matches should coincide in the center of the plots. This is, generally speaking, the case for free viewing except when reach and coherence are traded off (green direction). On the other hand, in most cases peripheral viewing is associated with matches shifted to lower reach and/or higher coherence compared to free viewing, indicative of a tendency toward image regularization.

emerged when observers modified both parameters in a correlated way. This might be due to observers being forced to trade off two opposing tendencies, toward sharper edges but regularized shapes. We notice, however, that in this condition observers were relatively biased when matching the stimuli in free viewing in the first place, indicating that this direction in parameter space might be particularly difficult for the observers. An idea of the relative task difficulty for the different directions in parameter space can be gained from the results of the discrimination experiment in Figure 7. It is quite evident that the just-noticeable differences in the directions where coherence and reach change in a correlated way are higher as compared to the case where they change in an anticorrelated way. This impression is confirmed by Wilcoxon paired signed-rank tests comparing the average just-noticeable differences in the northeast and southwest directions versus in the southeast and northwest directions (signed rank = 36, $p < 0.008$, for both natural and artificial images). This would not be expected if the perceptual effects of the parameter changes summed the same way independent of their signs.

Discussion

The first finding of our study is that observers are able to reliably navigate the space of the Eidolon Factory parameters to establish perceptual equivalence between central and peripheral vision. This confirms that the Eidolon Factory can be used as a tool to investigate the appearance of complex stimuli in the peripheral visual field. The main general finding of the study is that whenever observers exhibit a bias in matching the peripheral stimulus, they do so in terms of using lower reach and higher coherence, when exposed both to schematic combinations of shapes and to patches of relatively cluttered natural images. This means that the observers generally speaking reported the peripheral stimulus to be less distorted and less fuzzy, or sharper, than it actually was—that is, they tended to report the peripheral input to be closer to an unmodified image than it actually was.

The fact that such perceptual biases in peripheral vision exist might not require any strong functional explanation, since they might be functionally irrelevant.

Direction	Stimulus	Eccentricity	Signed rank	*p*
+Coherence	Artificial	20°	3	0.0024*
		30°	1.5	0.0014*
	Natural	20°	8	0.0061*
		30°	24	0.1464
+Coherence	Artificial	20°	60	0.1098
+Reach		30°	66	0.0341
	Natural	20°	70	0.0942
		30°	56	0.4973
+Reach	Artificial	20°	63	0.0605
		30°	57	0.1704
	Natural	20°	88	0.0012*
		30°	91	0.0002*
+Coherence	Artificial	20°	74.5	0.0029*
−Reach		30°	77	0.0009*
	Natural	20°	89	0.0007*
		30°	91	0.0002*

Table 1. Statistical analysis of the matching results. The signed rank and *p* values refer to a paired test between each observer's average matches during free fixation and at a given eccentricity, separately for each matching direction. *Notes*: The colors of the direction codes match the colors in Figures 2 and 6. Asterisks denote significant differences after false-discovery-rate correction (Benjamini & Yekutieli, 2001). *$p < 0.01$.

In our daily life we continuously move our gaze toward objects that we want to scrutinize, and one could argue that the main function of peripheral vision is to guide foveal selection rather than to support perception. Albeit speculative, one alternative way of looking at this phenomenon is to consider it one result of the predictive mechanisms that supplement the impoverished representation of our peripheral visual field, along with foveal-to-peripheral extrapolation (Otten et al., 2016; Toscani et al., 2017) and transsaccadic learning (Bosco et al., 2015; Herwig, 2015; Herwig et al., 2015; Valsecchi & Gegenfurtner, 2016; Weiß et al., 2014). The predictive nature of peripheral vision might subsume other phenomena such as the tendency to show liberal criteria for detecting peripheral targets (Solovey, Graney, & Lau, 2015) and the tendency to be overconfident in peripheral perceptual judgments (Li, Lau, & Odegaard, 2018; Odegaard, Chang, Lau, & Cheung, 2018). Such predictive mechanisms could be useful in reducing the perceptual discrepancy that we experience as we move our eyes.

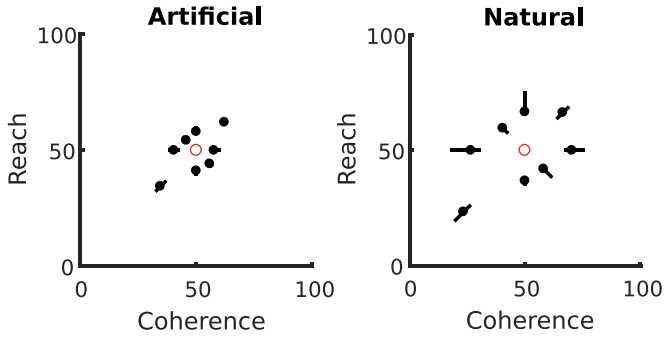

Figure 7. Detection thresholds for all eight directions and both types of stimuli. Values are expressed relative to the 100 steps that constitute the gamut of both parameters. The lines represent the 25th and 75th percentiles of the individual-observer values; the circles represent the median value. The thresholds for the cases where the two parameters change coherently (northeast and southwest) are larger than the ones where the two parameters change in an anticorrelated fashion (northwest and southeast). This confirms that correlated changes in the parameters are difficult for the observers to process. Notice that the physical reach of the standard stimuli is smaller for the natural images, so that the threshold values cannot be compared directly between artificial and natural stimuli.

The need for a functional explanation for the biases we observed in peripheral appearance is also underlined by the fact that peripheral vision has a specific role in blur perception. When it comes to perceiving the overall level of blur in a scene, peripheral and foveal input is integrated, so that adding peripheral information can generate a general impression of lower blur (Venkataraman, Radhakrishnan, Dorronsoro, Lundström, & Marcos, 2017), consistent with the phenomenon of sharpness overconstancy reported by Galvin and colleagues (Galvin et al., 1997; Galvin et al., 1999). Sharpness overconstancy is very reminiscent of our finding of increased peripheral coherence. Galvin and colleagues found that observers reported the sharpness of peripheral edges to be higher than it actually was. They interpreted this form of overconstancy as an indication that the appearance of a peripheral edge, given the inability to identify the correct level of blur in peripheral vision, is integrated with the template for a sharp edge. Such a template would originate from our experience of foveal viewing. With our study we demonstrate that this tendency to assume a reduced level of blur is not limited to the case of geometric shapes defined by sharp edges but, at least for the relatively near periphery, extends to cluttered natural stimuli.

Of course, we do not want to imply that predictive mechanisms in peripheral vision only determine the perceptual quality of edges. Multiple other templates, at different levels of abstraction, might be active simultaneously. One example that comes to mind is mirror symmetry, which is also hard to discriminate in peripheral vision (Barrett, Whitaker, McGraw, & Herbert, 1999). Particularly for categories of stimuli which are known to be mirror symmetric, such as faces, it is conceivable that observers will tend to report peripheral stimuli to be more symmetric than they actually are. It does not appear, however, that this tendency to regularization and simplification is universal, as is already evidenced by the fact that observers

tend to report circles to be elliptical in peripheral vision (Baldwin et al., 2016).

While we believe that the Eidolon Factory is a useful tool for studying peripheral appearance, it does have some limitations. One in particular has to do with the fact that the meaning of its parameters is defined within the context of the algorithm. Although they are related to different aspects which are definitely relevant to peripheral appearance—positional uncertainty for reach and blur for coherence—their effect is not independent both physically and perceptually. Physically, the effect of the coherence parameter on the resulting eidolon is dependent on the reach level, because if reach is low, the difference between images produced with low and high coherence is also reduced. At a reach of 0, the resulting eidolon is identical to the original image and coherence has no effect at all. Perceptually, the results of the discrimination experiment that we conducted show that if reach and coherence are modified in a correlated fashion—that is, they both increase or decrease—the resulting change tends to be less visible than if they change in an anticorrelated fashion. The particular difficulty of detecting correlated changes in reach and coherence, which we found in the discrimination experiment, possibly explains why observers tended to produce relatively biased matches already in foveal vision when they increased or decreased both reach and coherence in a correlated fashion. Having larger thresholds when reach and coherence were modified in a correlated fashion, and maximally large when both decrease, indicates that the section of the space where the stimuli appear identical is shifted in the direction of that pole.

This might not, however, be the only explanation for the foveal bias. Part of it might be dependent on the perceived magnitude or saliency of the suprathreshold perceptual changes associated with moving along the axes of the Eidolon Factory parameter space, which could also be asymmetric. On a higher level, observers might evaluate the changes that take place moving toward one of the two poles in a qualitatively different way. For instance, movement toward higher coherence and reach could be mostly appreciated as the emergence of large-scale distortions, whereas movement toward lower reach and coherence might be seen as a limited reduction in fuzziness (compare Figure 3), and the latter could be weighted much less. Generally speaking, one question that remains open for future research is whether perceptual dimensions can be established within the space of the Eidolon Factory parameters—that is, drawing iso-distortion and iso-fuzziness curves—so as to allow for an easier interpretation of biased reports about peripheral appearance.

Another possibility for further advancement of the present line of research is related to the functional interpretation of the biases we observed. It seems plausible to assume that the tendency to perceive sharp and straight edges in the periphery originates in our experience of foveal vision. We know that peripheral appearance can be influenced by learned associations between peripheral and foveal stimulation (Bosco et al., 2015; Herwig et al., 2015; Herwig & Schneider, 2014; Valsecchi & Gegenfurtner, 2016). Nonetheless, specific experiments will be needed to prove that this is the case. One testable prediction is that when a template for fuzzy borders is more appropriate—for instance if the peripheral stimulation depicts shadows cast under a relatively extended light source—observers might prefer to adjust them as being less sharp. Similarly, observers might have a template against straight edges when looking at images or movies of flames or flowing liquids, so that they might match them with higher reach when reporting their peripheral appearance.

In general, the base stimuli we used for our study—superimposed geometric shapes and patches from forest images—by no means exhaust the possible stimuli that could be investigated. For instance, it seems plausible to expect that the tendency toward regularization will be present for scenes of intermediate complexity, since we found it for both very simple and very complex stimuli. But to be certain one would need to test it directly using scenes with lower clutter, for instance indoor scenes. Also, our stimuli are generally dominated by large-scale structures, such as shapes, trees, and branches. It would be interesting to test whether our findings extend to images of textures, artificial and natural, where such structural elements are missing.

Considering the overall results of our study, we can try to list the advantages and disadvantages that using the Eidolon Factory shows relative to other approaches to investigating appearance in peripheral vision. We can classify those approaches into mainly three classes:

- Image-reproduction techniques such as verbal descriptions and drawing (Baldwin et al., 2016; Coates et al., 2017; Lettvin, 1976; Metzger, 1936, 2006; Sayim & Wagemans, 2017);
- Image/texture-synthesis techniques (Portilla & Simoncelli, 2000);
- Image-manipulation techniques such as band-pass noise warping (Bex, 2010) and low-pass filtering (Galvin et al., 1997).

The main advantages of the Eidolon Factory relative to image-reproduction techniques are that it can be applied to images of any complexity and it is easy to use in experiments with untrained observers because the images are changed parametrically.

The main advantage relative to synthesis techniques is again one of generality, because algorithms like that of Portilla and Simoncelli (2000) were mainly developed for texture synthesis. That algorithm extracts a

global, statistical representation of the image, which can then be used to generate other stimuli defined by the same statistical constraints. Using those models with stimuli that are not by nature translation invariant, such as scenes or depictions of objects, requires either limiting the spatial scope of the pooling of statistics (Freeman & Simoncelli, 2011)—that is, making the representation less global—or steering the synthesis toward the original stimulus. The Eidolon Factory instead relies on a scale-space representation of the stimulus which is both complete, in the sense that all the information necessary to reproduce the stimulus is encoded, and local. Having such a representation allows for perturbations to be applied selectively at any spatial scale and at any spatial location within a stimulus.

The main advantage relative to other image-manipulation techniques that have been used up to now is again that the Eidolon Factory is more general. Both band-pass noise warping and low-pass filtering are special subsets of the manipulations that can be obtained with the Eidolon Factory (band-pass noise warping is equivalent to full-coherence warping, and blurring can be produced by reweighting the different scale representations without applying warping before the eidolon is reassembled). However, the Eidolon Factory can produce a much larger range of visual effects which can be used to investigate perception. More importantly, scale-space representation is a fundamental structural property of the visual system, where input from each retinal location is encoded by means of receptive fields of different sizes. This suggests that manipulating a scale-space representation of the image is more appropriate than manipulating the image itself.

The main disadvantage relative to image-reproduction techniques is that using the Eidolon Factory limits the space of the effects that can be discovered in peripheral appearance. The parameter space of the Eidolon Factory defines the gamut of the stimuli that can be used for matching, whereas in reproduction experiments the limit is only the drawing or verbal ability of the participant. This disadvantage is common to image synthesis and to other image-manipulation techniques as well.

One possible advantage of the image-synthesis approach could again reside in the statistical nature of the image representation that it uses to generate stimuli. Using such a representation in principle allows for the generation of images that at some level of description are hybrid between different stimuli, which in turn might be useful for understanding what drives recognition in peripheral vision. Creating stimulus hybrids is much less straightforward when images are represented locally, as they are in the Eidolon Factory.

Finally, the main disadvantage relative to other image-manipulation techniques is definitely the difficulty of identifying perceptual dimensions within the Eidolon Factory parameter space. The perceptual effects of band-pass noise and blurring are likely much more orthogonal than the one of manipulating reach and coherence in an eidolon produced with scale decomposition.

Overall, each method has pros and cons. We believe that only through the convergence of the results obtained with different methods can both the specificity and generality of a given result be warranted.

To summarize the overall results of our study: Despite the fact that acuity loss and positional uncertainty reduce the reliability of the information we receive from our peripheral visual field, our visual world appears relatively homogeneous and integrated. We speculate that this is at least in part due to the fact that predictive mechanisms regularize the appearance of what we see in the periphery, driving it closer to the appearance that we experience in the fovea.

Keywords: peripheral appearance, Eidolon Factory, positional uncertainty, blur

Acknowledgments

MV and KG were supported by the SFB TRR 135 grant from the Deutsche Forschungsgemeinschaft. JK was supported by a Humboldt-Award from the Alexander-von-Humboldt-Foundation. We are grateful to Shin'ya Nishida for his comments and suggestions on an earlier version of this work. Data pertaining to this article are publicly available at https://doi.org/10.5281/zenodo.1490091.

Commercial relationships: none.
Corresponding author: Matteo Valsecchi.
Email: matteo.valsecchi@psychol.uni-giessen.de.
Address: Abteilung Allgemeine Psychologie, Justus-Liebig-Universität Giessen, Giessen, Germany.

References

Balas, B. (2016). Seeing number using texture: How summary statistics account for reductions in perceived numerosity in the visual periphery. *Attention, Perception, & Psychophysics*, *78*(8), 2313–2319, https://doi.org/10.3758/s13414-016-1204-6.

Balas, B., Nakano, L., & Rosenholtz, R. (2009). A summary-statistic representation in peripheral vi-

sion explains visual crowding. *Journal of Vision*, *9*(12):13, 1–18, https://doi.org/10.1167/9.12.13. [PubMed] [Article]

Baldwin, J., Burleigh, A., Pepperell, R., & Ruta, N. (2016). The perceived size and shape of objects in peripheral vision. *i-Perception*, *7*(4), 1–23, https://doi.org/10.1177/2041669516661900.

Barrett, B. T., Whitaker, D., McGraw, P. V., & Herbert, A. M. (1999). Discriminating mirror symmetry in foveal and extra-foveal vision. *Vision Research*, *39*(22), 3737–3744, https://doi.org/10.1016/S0042-6989(99)00083-8.

Benjamini, Y., & Yekutieli, D. (2001). The control of the false discovery rate in multiple testing under dependency. *The Annals of Statistics*, *29*(4), 1165–1188, https://doi.org/10.1214/aos/1013699998.

Bex, P. J. (2010). (In) Sensitivity to spatial distortion in natural scenes. *Journal of Vision*, *10*(2):23, 1–15, https://doi.org/10.1167/10.2.23. [PubMed] [Article]

Bosco, A., Lappe, M., & Fattori, P. (2015). Adaptation of saccades and perceived size after trans-saccadic changes of object size. *The Journal of Neuroscience*, *35*(43), 14448–14456, https://doi.org/10.1523/JNEUROSCI.0129-15.2015.

Boyadzhiev, I., Bala, K., Paris, S., & Adelson, E. (2015). Band-sifting decomposition for image-based material editing. *ACM Transactions on Graphics*, *34*(5), 163, https://doi.org/10.1145/2809796.

Clarke, A. D. F., Green, P. R., & Chantler, M. J. (2012). The effects of display time and eccentricity on the detection of amplitude and phase degradations in textured stimuli. *Journal of Vision*, *12*(3):7, 1–11, https://doi.org/10.1167/12.3.7. [PubMed] [Article]

Coates, D. R., Wagemans, J., & Sayim, B. (2017). Diagnosing the periphery: Using the Rey–Osterrieth Complex Figure drawing test to characterize peripheral visual function. *i-Perception*, *8*(3), 2041669517705447, https://doi.org/10.1177/2041669517705447.

Freeman, J., & Simoncelli, E. P. (2011). Metamers of the ventral stream. *Nature Neuroscience*, *14*, 1195–1201.

Galvin, S. J., O'Shea, R. P., Squire, A. M., & Govan, D. G. (1997). Sharpness overconstancy in peripheral vision. *Vision Research*, *37*(15), 2035–2039, https://doi.org/10.1016/S0042-6989(97)00016-3.

Galvin, S. J., O'Shea, R. P., Squire, A. M., & Hailstone, D. S. (1999). Sharpness overconstancy: The roles of visibility and current context. *Vision Research*, *39*(16), 2649–2657, https://doi.org/10.1016/S0042-6989(98)00306-X.

Ganmor, E., Landy, M. S., & Simoncelli, E. P. (2015). Near-optimal integration of orientation information across saccades. *Journal of Vision*, *15*(16):8, 1–12, https://doi.org/10.1167/15.16.8. [PubMed] [Article]

Giesel, M., & Zaidi, Q. (2013). Frequency-based heuristics for material perception. *Journal of Vision*, *13*(14):7, 1–19, https://doi.org/10.1167/13.14.7. [PubMed] [Article]

Herwig, A. (2015). Transsaccadic integration and perceptual continuity. *Journal of Vision*, *15*(16):7, 1–6, https://doi.org/10.1167/15.16.7. [PubMed] [Article]

Herwig, A., & Schneider, W. X. (2014). Predicting object features across saccades: Evidence from object recognition and visual search. *Journal of Experimental Psychology: General*, *143*(5), 1903–1922.

Herwig, A., Weiß, K., & Schneider, W. X. (2015). When circles become triangular: How transsaccadic predictions shape the perception of shape. *Annals of the New York Academy of Sciences*, *1339*(1), 97–105.

Hilz, R., & Cavonius, C. R. (1974). Functional organization of the peripheral retina: Sensitivity to periodic stimuli. *Vision Research*, *14*(12), 1333–1337, https://doi.org/10.1016/0042-6989(74)90006-6.

Itti, L., & Koch, C. (2000). A saliency-based search mechanism for overt and covert shifts of visual attention. *Vision Research*, *40*(10), 1489–1506, https://doi.org/10.1016/S0042-6989(99)00163-7.

Johnston, A. (1987). Spatial scaling of central and peripheral contrast-sensitivity functions. *Journal of the Optical Society of America A*, *4*(8), 1583–1593, https://doi.org/10.1364/JOSAA.4.001583.

Keshvari, S., & Rosenholtz, R. (2016). Pooling of continuous features provides a unifying account of crowding. *Journal of Vision*, *16*(3):39, 1–15, https://doi.org/10.1167/16.3.39. [PubMed] [Article]

Keshvari, S., & Wijntjes, M. (2016). Peripheral material perception. *Journal of Vision*, *16*(12): 641, https://doi.org/10.1167/16.12.641. [Abstract]

Koenderink, J., Valsecchi, M., van Doorn, A., Wagemans, J., & Gegenfurtner, K. (2017). Eidolons: Novel stimuli for vision research. *Journal of Vision*, *17*(2):7, 1–36, https://doi.org/10.1167/17.2.7. [PubMed] [Article]

Lettvin, J. (1976). On seeing sidelong. *The Sciences*, *16*(4), 10–20, https://doi.org/10.1002/j.2326-1951.1976.tb01231.x.

Levi, D. M. (2008). Crowding—An essential bottleneck

for object recognition: A mini-review. *Vision Research*, *48*(5), 635–654, https://doi.org/10.1016/j.visres.2007.12.009.

Li, M. K., Lau, H., & Odegaard, B. (2018). An investigation of detection biases in the unattended periphery during simulated driving. *Attention, Perception, & Psychophysics*, *80*(6), 1325–1332, https://doi.org/10.3758/s13414-018-1554-3.

Maiello, G., Walker, L., Bex, P. J., & Vera-Diaz, F. A. (2017). Blur perception throughout the visual field in myopia and emmetropia. *Journal of Vision*, *17*(5):3, 1–13, https://doi.org/10.1167/17.5.3. [PubMed] [Article]

Martinez-Conde, S., Macknik, S. L., Troncoso, X. G., & Dyar, T. A. (2006). Microsaccades counteract visual fading during fixation. *Neuron*, *49*(2), 297–305, https://doi.org/10.1016/j.neuron.2005.11.033.

Metzger, W. (1936). *Gesetze des Sehens* [Laws of seeing]. Frankfurt, Germany: Waldemar Kramer.

Mostofi, N., Boi, M., & Rucci, M. (2016). Are the visual transients from microsaccades helpful? Measuring the influences of small saccades on contrast sensitivity. *Fixational Eye Movements and Perception*, *118*, 60–69, https://doi.org/10.1016/j.visres.2015.01.003.

Newsome, L. R. (1972). Visual angle and apparent size of objects in peripheral vision. *Perception & Psychophysics*, *12*(3), 300–304, https://doi.org/10.3758/BF03207209.

Odegaard, B., Chang, M. Y., Lau, H., & Cheung, S.-H. (2018). Inflation versus filling-in: Why we feel we see more than we actually do in peripheral vision. *Philosophical Transactions of the Royal Society B: Biological Sciences*, 373: 20170345, 1–10, https://doi.org/10.1098/rstb.2017.0345.

Otero-Millan, J., Macknik, S. L., Langston, R. E., & Martinez-Conde, S. (2013). An oculomotor continuum from exploration to fixation. *Proceedings of the National Academy of Sciences, USA*, *110*(15), 6175–6180, https://doi.org/10.1073/pnas.1222715110.

Otten, M., Pinto, Y., Paffen, C. L. E., Seth, A. K., & Kanai, R. (2016). The uniformity illusion: Central stimuli can determine peripheral perception. *Psychological Science*, *28*(1), 56–68, https://doi.org/10.1177/0956797616672270.

Portilla, J., & Simoncelli, E. P. (2000). A parametric texture model based on joint statistics of complex wavelet coefficients. *International Journal of Computer Vision*, *40*(1), 49–70, https://doi.org/10.1023/A:1026553619983.

Rosenholtz, R. (2016). Capabilities and limitations of peripheral vision. *Annual Review of Vision Science*, *2*, 437–457.

Sayim, B., Myin, E., & Van Uytven, T. (2015, May). *Prior knowledge modulates peripheral color appearance*. Presented at the Midterm Meeting of the International Colour Association, Tokyo, Japan.

Sayim, B., & Wagemans, J. (2017). Appearance changes and error characteristics in crowding revealed by drawings. *Journal of Vision*, *17*(11):8, 1–16, https://doi.org/10.1167/17.11.8. [PubMed] [Article]

Solovey, G., Graney, G. G., & Lau, H. (2015). A decisional account of subjective inflation of visual perception at the periphery. *Attention, Perception, & Psychophysics*, *77*(1), 258–271, https://doi.org/10.3758/s13414-014-0769-1.

Strasburger, H., Rentschler, I., & Jüttner, M. (2011). Peripheral vision and pattern recognition: A review. *Journal of Vision*, *11*(5):13, 1–82, https://doi.org/10.1167/11.5.13. [PubMed] [Article]

Tkačik, G., Garrigan, P., Ratliff, C., Milčinski, G., Klein, J. M., Seyfarth, L. H., ... Balasubramanian, V. (2011). Natural images from the birthplace of the human eye. *PLoS One*, *6*(6), e20409, https://doi.org/10.1371/journal.pone.0020409.

Toscani, M., Gegenfurtner, K. R., & Valsecchi, M. (2017). Foveal to peripheral extrapolation of brightness within objects. *Journal of Vision*, *17*(9):14, 1–14, https://doi.org/10.1167/17.9.14. [PubMed] [Article]

Valsecchi, M., & Gegenfurtner, K. R. (2016). Dynamic re-calibration of perceived size in fovea and periphery through predictable size changes. *Current Biology*, *26*(1), 59–63, https://doi.org/10.1016/j.cub.2015.10.067.

Valsecchi, M., Toscani, M., & Gegenfurtner, K. R. (2013). Perceived numerosity is reduced in peripheral vision. *Journal of Vision*, *13*(13):7, 1–16, https://doi.org/10.1167/13.13.7. [PubMed] [Article]

Venkataraman, A. P., Radhakrishnan, A., Dorronsoro, C., Lundström, L., & Marcos, S. (2017). Role of parafovea in blur perception. *Vision Research*, *138*, 59–65, https://doi.org/10.1016/j.visres.2017.07.005.

Wallis, T. S. A., Bethge, M., & Wichmann, F. A. (2016). Testing models of peripheral encoding using metamerism in an oddity paradigm. *Journal of Vision*, *16*(2):4, 1–30, https://doi.org/10.1167/16.2.4. [PubMed] [Article]

Wang, B., Ciuffreda, K. J., & Irish, T. (2006). Equiblur zones at the fovea and near retinal periphery. *Vision*

Research, *46*(21), 3690–3698, https://doi.org/10.1016/j.visres.2006.04.005.

Weiß, K., Schneider, W. X., & Herwig, A. (2014). Associating peripheral and foveal visual input across saccades: A default mode of the human visual system? *Journal of Vision*, *14*(11):7, 1–15, https://doi.org/10.1167/14.11.7. [PubMed] [Article]

Whitney, D., & Levi, D. M. (2011). Visual crowding: A fundamental limit on conscious perception and object recognition. *Trends in Cognitive Sciences*, *15*(4), 160–168, https://doi.org/10.1016/j.tics.2011.02.005.

Wolf, C., & Schütz, A. C. (2015). Trans-saccadic integration of peripheral and foveal feature information is close to optimal. *Journal of Vision*, *15*(16):1, 1–18, https://doi.org/10.1167/15.16.1. [PubMed] [Article]